

Topological Transitions in Liquid/Liquid Interfaces

J.S Lowengrub* J. Goodman[†] H. Lee[‡] E.K. Longmire[§]

M.J. Shelley[¶] L. Truskinovsky^{||}

March 14, 1998

1 Introduction

A set of fundamental yet ill-understood phenomena in fluid dynamics involves changes in the topology of interfaces between partially miscible or nominally 'immiscible' fluids. Such changes occur, for example, when continuous jets pinch off into droplets, when sheared interfaces atomize, and when droplets of one fluid reconnect with one another. These topological transitions occur in many practical applications involving transport, mixing, and separation of petroleum, chemical, and food products as well as contaminated waste streams.

The dynamics of topological transitions are difficult to understand and model for several reasons. For one, the fluids in which these transitions occur are complex. A second problem associated with topological transitions is caused by the short time scales over which they occur. In practical flows, the transition time scales are much shorter than the local flow time scales making the transitions difficult to characterize experimentally or compute numerically. A third problem associated with transitions is purely numerical: how does one handle the change in interface topology in a physically justified way? In this paper, we will address the last problem in the context of incompressible fluid flows.

Many researchers (see [16, 19] for example) have tried using ad hoc methods to change the topology of interfaces. While this approach, often referred to as "contour surgery," allows topological transitions to be overcome, it is difficult to justify the reconnection conditions based on physical principles. In a few special cases, involving fluid-gas interfaces, it is possible to develop physically-based reconnection conditions by using special similarity solutions of the Navier-Stokes equations (see [12, 4, 3]). For flows involving liquid/liquid interfaces, however, the dynamics are more complicated and no such similarity solutions have been constructed.

*Department of Mathematics, University of Minnesota, Minneapolis, MN 55455.

[†]Courant Institute, New York University New York, NY 10012.

[‡]Department of Mathematics, University of Minnesota, Minneapolis, MN 55455.

[§]Department of Aerospace and Mechanics, University of Minnesota Minneapolis, MN 55455.

[¶]Courant Institute, New York University New York, NY 10012.

^{||}Department of Aerospace and Mechanics, University of Minnesota Minneapolis, MN 55455.

In an attempt to derive a physically-based theory of sharp liquid/liquid interfaces near topological transitions, several researchers (see [1, 2, 18] for example) have proposed representing the interface as the level set of a higher-order function. Thus different level sets (or fixed values of the function) could exhibit different topologies. In this approach, the interface is effectively given a finite thickness by smoothing the flow discontinuities (density, viscosity) over a narrow region. Although this procedure generally yields a smooth evolution through topological changes, one can demonstrate that the results can depend essentially on the type of smoothing chosen [15]. Within the context of this “level set” method, it is not clear *which* types of smoothing are physically justified.

Three of the authors (JG, JL, and MS) have proposed an alternative; introduce an explicit order parameter (e.g. concentration) and allow limited mixing across the interfacial zone. In this approach, the sharp interface is replaced by a smooth, narrow transition layer (in the order parameter) and the resulting system consists of the Navier-Stokes (NS) equations coupled to either a Ginzburg-Landau (nonconserved, GL) or Cahn-Hilliard (conserved, CH) equation for the order parameter. Gradients in the parameter produce reactive stresses in the fluid which mimic surface tension. The above authors gave a physical derivation of the equations in a special case (models of type E and H in the nomenclature of Hohenberg & Halperin [8]). Subsequently, Lowengrub & Truskinovsky in [15] gave a more general and systematic derivation of the equations, with the conserved mass concentration as the order parameter, and gave an analysis of the equations in some special cases including a simple model of a topology transition.

Here, the mass concentration is the physically relevant order parameter and the limited mixing is due to chemical diffusion between the different fluids. In physical chemistry, it is well known that limited molecular mixing occurs between macroscopically “immiscible” fluids. This limited mixing provides a *physical mechanism* to smooth the flow discontinuities and to yield smooth evolutions through topological changes. Thus, the NS-CH system can be viewed as a partial miscibility regularization (PMR) of the sharp interface model.

In this paper, we present preliminary numerical results using the PMR model in two interfacial flow regimes: (1). viscously dominated flows in Hele-Shaw cells (unstably stratified fluid layers), and (2). 2-d inertially dominated flows (liquid/liquid jets). In both cases, topological transitions are smoothly captured by the PMR model. Vorticity is produced at the pinchoff point and the interfaces ‘snap’ back after the transition. In the Hele-Shaw case, the vorticity remains bound to the interface through the transition. This suggests that it may be possible to use the PMR to formulate ‘topological jump conditions’ to reconnect sharp interfaces within the context of a boundary integral simulation, for example. This is currently under investigation. In the inertially dominated case, simulations of inviscid liquid/liquid jets show that some vorticity *separates* from the interface after pinchoff and there is a nontrivial flow inside the newly created drops. In both cases before pinchoff, the results show good agreement with boundary integral simulations.

2 Equations of Motion

We begin our presentation of the PMR equations by first reviewing the classical theory of surface tension. Let two immiscible, incompressible fluids be separated by a sharp interface Γ and let

$\Gamma = \{x|\phi(x, t) = 0\}$ where $\phi > 0$ denotes the region with fluid 1 and $\phi < 0$ denotes the region with fluid 2. Then, one can introduce the characteristic function χ of the fluid 1 region by

$$\chi(\phi) = H(\phi) = \begin{cases} 1 & \text{if } \phi > 0, \\ 0 & \text{otherwise} \end{cases} \quad (1)$$

where H is the Heaviside function. One can then define the fluid quantities in terms of χ . For example, let the density $\rho = \rho_1\chi(\phi) + \rho_2(1 - \chi(\phi))$ where ρ_1 and ρ_2 are the constant densities of fluids 1 and 2 respectively. The other material parameters are defined analogously. The mass and momentum balance equations are given by

$$\nabla \cdot \mathbf{u} = 0 \quad \text{and} \quad \dot{\phi} = 0, \quad (2)$$

$$\rho \dot{\mathbf{u}} = \nabla \cdot \mathbf{P}, \quad \text{and} \quad \mathbf{P} = -p\mathbf{I} - \sigma(\mathbf{n} \otimes \mathbf{n} - \mathbf{I})\delta_\Gamma + 2\nu\mathbf{D} \quad (3)$$

where $\dot{\cdot} = \partial_t + \mathbf{u} \cdot \nabla$ is the advective time derivative, p is the pressure, σ is the surface tension, $\mathbf{n} = \nabla\phi/|\nabla\phi|$ is the normal vector to Γ , δ_Γ is the surface delta function, $\nu = \nu(\phi)$ is the viscosity and $\mathbf{D} = (\nabla\mathbf{u} + \nabla\mathbf{u}^T)/2$ is rate of strain tensor. As is well known, the surface delta function can be related to the 1-d delta function δ by $\delta_\Gamma = \delta(\phi)|\nabla\phi|$. This formulation (2)-(3) guarantees that the classical boundary conditions

$$[\mathbf{u} \cdot \mathbf{n}]_1^2 \equiv \mathbf{u} \cdot \mathbf{n}|_2 - \mathbf{u} \cdot \mathbf{n}|_1 = 0, \quad V = \mathbf{u} \cdot \mathbf{n}|_\Gamma \quad (4)$$

$$[\mathbf{P} \cdot \mathbf{n}]_1^2 = 2\sigma\kappa \quad (5)$$

hold across Γ . In the above, V is the normal velocity of Γ and κ is its mean curvature.

The solutions to Eqs. (2)-(3) generically develop singularities in both 2 and 3 dimensions. These singularities typically develop due to topological changes in the flow such as the collision of material interfaces Γ . When material surfaces collide, or self-intersect, velocity gradients necessarily diverge [10] and the curvature tends to blow-up as well. For 2-d, see [9, 10]. In 3-d, it is the classical Rayleigh instability that drives the singularity formation.

To bridge the transition and continue the flow beyond the singularity, one has several choices. One can deal directly with the equations (2)-(3) and try to obtain and match similarity solutions as was done in [3] for liquid/gas interfaces or one can regularize the equations. Here, we follow the latter approach.

The simplest regularization of the sharp interface Eqs. (2)-(3) is to smooth $\chi \rightarrow \chi_\epsilon$ and $\delta_\Gamma \rightarrow \delta_\Gamma^\epsilon$. For example, one can set

$$\delta_\Gamma^\epsilon = \epsilon|\nabla\phi|(\chi'_\epsilon)^2 \quad \text{with} \quad \sigma = \lim_{\epsilon \rightarrow 0} \int_{-\infty}^{+\infty} \epsilon[\chi'_\epsilon(\phi)]^2 d\phi. \quad (6)$$

Then, one can repose Eq. (3) using the smoothed stress tensor \mathbf{P}^ϵ . This method is basically the level set method described in [1, 2, 18, 17]. While this method yields smooth evolutions through topology changes, in our view, there are several potential drawbacks. First, it is the numerical diffusion, which is fluid-independent, that actually controls the reconnection process and yields the smooth evolution through the topology change. Second, the solutions can depend essentially on the type of smoothing (see [15] for an explicit example for spherical drops). Thus, while we can imagine χ_ϵ as an artificial concentration field, there is no physical chemistry in this model.

2.1 Navier-Stokes-Cahn-Hilliard Equations

One can try to account for the physical chemistry by introducing a mass concentration field $c = M_1/M$ which is conserved, consistently coupled to the fluid equations and evolves according to a diffusion equation; this is the PMR. A derivation of the equations is given in [15] and we only present the nondimensional result here:

$$\rho_0 \dot{c} = \frac{1}{\mathbf{Pe}} \Delta \mu, \quad \nabla \cdot \mathbf{u} = \frac{\alpha}{\mathbf{Pe}} \Delta \mu \quad (7)$$

$$(8)$$

$$\rho_0 \dot{\mathbf{u}} = -\frac{1}{\mathbf{M}} [\nabla p + \mathbf{C} \nabla \cdot (\rho_0 \nabla c \otimes \nabla c)] + \frac{1}{\mathbf{Re}} \nabla \cdot [2\eta(c)\mathbf{D}] + \frac{1}{\mathbf{Fr}} \rho_0 \mathbf{g} \quad (9)$$

where $\rho_0 = \rho_0(c)$ is the simple mixture density [11] defined by $1/\rho_0(c) = c/\rho_1 + (1-c)/\rho_2$, μ is the chemical potential

$$\mu = \frac{df_0}{dc}(c) - \frac{\rho'_0}{\rho_0^2} p - \frac{\mathbf{C}}{\rho_0} \nabla \cdot (\rho_0 \nabla c) \quad (10)$$

and \mathbf{C} is the Cahn number which is a measure of the interface thickness and $f_0(c)$ is a non-convex, non-negative function. \mathbf{Pe} is the diffusional Peclet number, $\alpha = 1/\rho_1 - 1/\rho_2$ is a constant, \mathbf{M} is a generalized Mach number, \mathbf{Re} is a Reynolds number, \mathbf{Fr} is a Froude number and \mathbf{g} is unit vector pointing in the direction of the gravitational field. We refer the reader to [15] for explicit definitions of these nondimensional quantities.

We remark in the density-matched case $\rho_1 = \rho_2$, Eqs. (7)-(10) reduce to Model H given in [8]. The equation for c is a 4th order diffusion equation of Cahn-Hilliard type. Eq. (9) is a generalization of the Navier-Stokes equation in which gradients in c produce reactive stresses in the fluid which mimic surface tension. We refer to this as the NSCH system. It is interesting to note that if $\rho_1 \neq \rho_2$, then diffusion creates density variation so that $\nabla \cdot \mathbf{u} \neq 0$ which introduces compressibility effects even when the original fluids are incompressible. We refer to this case as *quasi-incompressible*. The pressure also explicitly appears in the chemical potential. Some consequences of this are discussed in [15]. Finally, Eqs. (7)-(10) have an associated non-increasing energy functional which is the sum of the kinetic, potential and chemical energies.

In [15], the sharp interface limit of (7)-(10) was discussed using matched asymptotic expansions. We present the result here. Let γ be a small parameter that measures the thickness of the interface and let $\mathbf{C} = \gamma^2$, $\mathbf{M} = \gamma$ and $\mathbf{Pe} = 1/\gamma$. Then, if the mean curvature $\kappa \ll 1/\gamma$, the system (7)-(10) converges to the sharp interface system (2)-(3) with ϕ replaced by c , $\Gamma = \{\mathbf{x} \mid c(\mathbf{x}, t) = 1/2\}$ and the surface tension given by

$$\sigma = \int_0^1 \rho_0(c) \sqrt{2f_0(c)} dc \quad (11)$$

In this paper, we always use $f_0(c) = Ac^2(1-c)^2/4$ and use A to match the sharp interface surface tension.

2.2 Hele-Shaw-Cahn-Hilliard Equations

We next present the PMR model appropriate for quasi-incompressible binary fluids in a Hele-Shaw cell. A Hele-Shaw cell consists of two parallel plates separated by a narrow gap. The flow takes place in the gap and it is assumed that the fluids are highly viscous so that inertial effects are negligible. In addition, because the gap between the plates is narrow, the flow is only weakly three-dimensional. Our primary motivation for discussing and eventually studying this flow is that it is much simpler mathematically and physically than the general NSCH system and therefore provides an excellent case for testing the effects of parametric variations.

The sharp interface formulation is as follows. In each fluid domain, the velocity is given by Darcy's law:

$$\mathbf{u}_i = -\frac{1}{12\eta_i} [\nabla p - \rho_i \mathbf{g}], \quad \text{in } \Omega_i \quad (12)$$

and the fluids are incompressible $\nabla \cdot \mathbf{u}_i = 0$ for $i = 1, 2$. The boundary conditions across the interface $\Gamma = \partial\Omega_1 \cap \partial\Omega_2$ are exactly as in (4) and (5).

In recent work, Lee & Lowengrub [13] derived the PMR appropriate for flow in a Hele-Shaw cell. In this case, the equations are referred to as the Hele-Shaw-Cahn-Hilliard (HSCH) system and are given by

$$\rho_0 \dot{c} = \gamma \Delta c, \quad \nabla \cdot \mathbf{u} = \alpha \gamma \Delta c \quad (13)$$

$$\mathbf{u} = -\frac{1}{12\nu(c)} [\nabla p + \gamma \nabla \cdot (\rho_0 \nabla c \otimes \nabla c) - \rho_0 \mathbf{g}] \quad (14)$$

$$\mu = \frac{df_0}{dc}(c) + \alpha \gamma p - \frac{1}{\rho_0} \nabla \cdot (\gamma^2 \rho_0 \nabla c) \quad (15)$$

where \mathbf{u} and c are the gap-averaged velocity and concentration fields respectively (2 dimensional), ∇ is the two dimensional gradient and \mathbf{g} is gravity. Note that the gap width has been scaled out of the formulation and that we have explicitly used the sharp interface scaling as described in the previous section.

There are three important parameters in the HSCH model. There is the Bond number $\mathbf{B} = g(\rho_1 - \rho_2)/\sigma$, the Atwood number for viscosity $\mathbf{A}_\nu = (\nu_1 - \nu_2)/(\nu_1 + \nu_2)$ and the interface thickness γ .

This system is much simpler than the NSCH equations. There is no dynamical equation for the velocity \mathbf{u} ; the velocity is determined through a generalized Darcy's law (14). Once c is determined, then \mathbf{u} is found by solving Eqs. (13)b and (14). Nevertheless, there are still many common features with the NSCH model. In particular, the compressibility effects due to chemical diffusion are still present. As in the NSCH case, it can be shown [13] that as $\gamma \rightarrow 0$, the system (13)-(15) converges to the sharp interface equations with surface tension σ given by Eq. (12).

3 Results

In this section, we present preliminary numerical results for the HSCH and NSCH models. We begin by considering thin, unstably stratified layers in a Hele-Shaw cell.

3.1 HSCH Simulations

Let us suppose that $\rho_1 - \rho_2 \ll 1$ but $g(\rho_1 - \rho_2) = O(1)$. Then, we can assume ρ_0 is constant in the equations everywhere except in the gravitational term where we take ρ_0 to be a linear function of c . This is a Boussinesq approximation and there are no compressibility effects in this limiting case. In the simulations we present here, we use this approximation of the HSCH equations and we further set $A_\nu = 0$ so that the fluids are viscosity matched. More complicated scenarios are discussed in [13]. By considering this case first, we can isolate the effects of diffusion from those of compressibility.

For our numerical methods, we use periodic boundary conditions and pseudo-spectral spatial discretizations of Eqs. (13)-(15). We use a non-stiff time stepping algorithm to solve the concentration equation in Fourier space. In this approach, the equation is reformulated by using an integrating factor associated with the 4th order term in Fourier space. The reformulated equations are discretized using a 3rd order Adams-Bashforth method. See [13].

Now, consider an unstably stratified layer which consists of layer of light fluid surrounded by a heavy fluid. There are two interfaces; the upper interface is unstable while the lower interface is stable. We take $\mathbf{B} = 25$ for the upper interface and $\mathbf{B} = -25$ for the lower. A boundary integral simulation of the evolution is given in figure 1. Periodic boundary conditions are used and only 1 periodic box is shown. The simulation suggests that at a time slightly beyond $t = 7.7$, the layer pinches off at two points leaving the flow consisting of two large bubbles with a single narrow bubble in between. Flows of this type have been studied extensively both theoretically and numerically in [7, 6] and we refer the reader there for additional background.

We now repeat the flow using the HSCH model with $\rho_0 = 1 - 0.1c$. In addition, we use the reference frame of the sharp interface model. That is, a constant adverse pressure gradient (to the gravitational field) is introduced whose strength is equal to the mean density (in a single periodic box). With this pressure gradient, flat interfaces are motionless. The resulting simulation is shown in figure 2. Three x -periods are plotted. In the upper graphs, concentration is plotted and in the lower graphs, the vorticity is plotted. In this simulation, we have used $\gamma = 0.05$, $N = 256$ and $\Delta t = 10^{-3}$. There are approximately 8 computational points across the interface. The evolution smoothly passes through the topological change and the layer breaks up into droplets. Interestingly, there is a secondary break-up as the flat droplet splits into three small ‘round’ drops. Oppositely-signed vorticity is produced at the pinching point and acts to ‘snap’ back the drop tips.

That vorticity is produced by the transition can be seen by considering the maximum vorticity as a function of time. This is shown in figure 3. The four graphs correspond to the four interface thicknesses $\gamma = 0.05$, $\gamma = 0.06$, $\gamma = 0.08$ and $\gamma = 0.10$. The second peak in the $\gamma = 0.05$ curve is due to the secondary pinch-off. The computations with larger γ do not exhibit this secondary

pinchoff and so only one peak is observed. In those computations, the diffusion smears those details enough so that only a single bubble is observed [13]. Note that the primary pinch-off time is a stable function of γ .

Finally, in figure 4, results from the sharp and HSCH models are compared. Good agreement is observed between the sharp interface (solid line) and the $c = 1/2$ contour line (dashed line) although the layer in the HSCH model pinches off slightly earlier.

3.2 NSCH Simulations

In this section, we present a single simulation of the break-up of a 2-d density-matched, inviscid jet using the NSCH model. We also compare the result to a sharp interface simulation.

As in the Hele-Shaw case, we use periodic boundary conditions and pseudo-spectral spatial discretization. The time-stepping for the both concentration and velocity equation uses 2nd order Adams-Bashforth. In the concentration equation, the integrating factor in Fourier space is used. In the velocity equation, high-order Fourier filtering is used to maintain stability [14].

We begin by comparing the results from a sharp interface simulation with those from the NSCH model. The surface tension $\sigma = 1/2$ and the jump in tangential velocity equals 1 across the upper interface and -1 across the lower interface. Thus, the flow inside the jet is from left to right. A time sequence of a single periodic box is shown in figure 5. Again, the solid curve is the sharp interface and the dashed curve is the $c = 1/2$ contour line for the NSCH simulation. The NSCH simulation uses $\rho_0 = 1$, $\gamma = 0.06$, $N = 256$; there are approximately 12 points across the interfacial zone.

Good agreement is seen between the two simulations although the NSCH jet pinches at a slightly later time than the sharp interface jet. In the picture on the lower right, a close-up of the pinching region is shown and an additional NSCH simulation using $\gamma = 0.04$ is included (dot-dashed curve) which suggests convergence to the sharp interface result.

The NSCH simulations continue smoothly through the pinching and the long-time evolution of this NSCH jet is shown in figure 6. Again, three x -periods are shown; the upper graphs are concentration and the lower graphs are vorticity. As in the Hele-Shaw case, oppositely-signed vorticity is produced at the pinching point, but now some vorticity separates from the concentration interface creating a complicated flow-field both inside and outside the newly created drops which oscillate in time as they travel from left to right through the flow.

4 Conclusions and Future Work

In this paper, we have presented two new systems of equations to describe the motion of binary fluids in 2-d inertially dominated flows and viscously dominated flows in a Hele-Shaw cell. We have solved these equations numerically and demonstrated that topology transitions are smoothly captured. Before pinchoff, there is good agreement with sharp interface models.

In the future, we will consider axisymmetric and 3-d flows, incorporate local grid refinement and adaptivity, consider compressibility effects. We will compare our results to those obtained using other models, such as the level set method, and to those from actual experiments of

liquid/liquid jets performed in E. Longmire's laboratory where quantified measurements will be made of velocity, vorticity and concentration. Preliminary experiments have already been performed and the results are encouraging [5].

5 Acknowledgements

J.S.L. and H.L. were supported in part by the National Science Foundation (NSF) Grants DMS-940310, DMS-9706931, the Sloan Foundation and the Minnesota Supercomputer Institute. J.G. acknowledges the support of the NSF and the Office of Naval Research. E.K.L. acknowledges the support of the NSF Grant CTS-9457014. M.J.S. acknowledges the support of the Department of Energy Grant DE-FG02-88ER25053, NSF Grants DMS-9396403 (PVI) and DMS-9404554 and the Exxon Educational Foundation. L.T. acknowledges the support of NSF Grant DMS-9501433.

References

- [1] J.U. Brackbill, D.B. Kothe, and C. Zemach. A continuum method for modeling surface tension. *J. Comp. Phys.*, 100:335, 1994.
- [2] Y.C. Chang, T.Y. Hou, B. Merriman, and S. Osher. A level set formulation of Eulerian interface capturing methods for incompressible fluid flows. *J. Comp. Phys.* in press.
- [3] J. Eggers. Theory of drop formation. *Phys. Fluids*, 7:941, 1995.
- [4] J. Eggers and T.F. Dupont. Drop formation in a one dimensional approximation of the Navier-Stokes equations. *J. Fluid Mech.*, 262:205, 1994.
- [5] E.K. Longmire, D. Webster, D. Gefroh and J.S. Lowengrub. Dynamics of pinch-off in liquid jets flowing into immiscible liquid ambients. In *Proceedings of Third International Conference on Multiphase Flow*. 1998.
- [6] R. Goldstein, A. Pesci, and M. Shelley. Instabilities and instabilities in Hele-Shaw flow. to appear *Phys. Fluids A*.
- [7] R. Goldstein, A. Pesci, and M. Shelley. Attracting manifold for a viscous topology transition. *Phys. Rev. Lett.*, 75:3665, 1995.
- [8] P.C. Hohenberg and B.I. Halperin. Theory of dynamic critical phenomena. *Rev. Mod. Phys.*, 49:435, 1977.
- [9] T.Y. Hou, J.S. Lowengrub, and M.J. Shelley. Removing the stiffness from interfacial flows with surface tension. *J. Comp. Phys.*, 114:312, 1994.
- [10] T.Y. Hou, J.S. Lowengrub, and M.J. Shelley. The long-time evolution of vortex sheets with surface tension. *Phys. Fluids A*, 9:1933, 1997.

- [11] D.D. Joseph. Fluid dynamics of two miscible liquids with diffusion and gradient stresses. *Eur. J. Mech. B/Fluids*, 9:565, 1990.
- [12] J. B. Keller and M. Miksis. Surface tension driven flows. *SIAM J. App. Math*, 43:268, 1983.
- [13] H. Lee and J.S. Lowengrub. Topological transitions in Hele-Shaw cells. in preparation.
- [14] J.S. Lowengrub, M.J. Shelley, J. Goodman, and L. Truskinovsky. Topological transitions in liquid/liquid jets. in preparation.
- [15] J.S. Lowengrub and L. Truskinovsky. Quasi-incompressible Cahn-Hilliard fluids and topological transitions. to appear Proc. R. Soc. London A.
- [16] N. Mansour and T. Lundgren. Satellite formation in capillary jet breakup. *Phys. Fluids A*, 2:1141, 1990.
- [17] M. Sussman and P. Smereka. Axisymmetric free boundary problems. *J. Fluid Mech.*, 341:269, 1997.
- [18] M. Sussman, P. Smereka, and S. Osher. A level set approach for computing solutions to incompressible two-phase flow. *J. Comp. Phys.*, 114:146, 1994.
- [19] S.O. Unverdi and G. Tryggvason. A front tracking method for viscous, incompressible multi-fluid flows. *J. Comp. Phys.*, 100:25, 1992.

6 Figure Captions

Figure 1: Boundary integral simulation with $\mathbf{B} = \pm 25$, $N = 1024$, $\Delta t = 5 \times 10^{-4}$.

Figure 2: HSCH simulation with $\mathbf{B} = \pm 25$, $\rho_0 = 1 - 0.1c$, $N = 256$ and $\Delta t = 10^{-3}$. Three x -periods are shown.

Figure 3: Maximum vorticity vs. time for HSCH simulation.

Figure 4: Comparison of sharp and HSCH simulations.

Figure 5: Comparison of sharp and NSCH simulations. The sharp interface method uses $N = 1024$, $\Delta t = 10^{-3}$, $\sigma = 1/2$. The NSCH model uses $\rho_0 = 1$, $\gamma = 0.06$ and $N = 256$.

Figure 6: Long-time simulation of the NSCH jet. Three x -periods are shown.

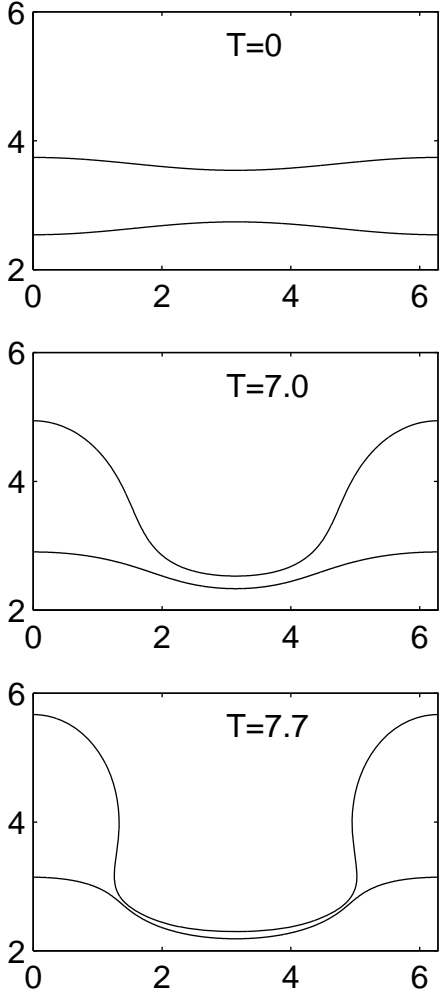


Figure 1:

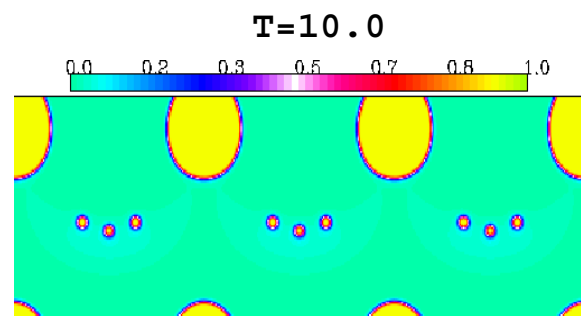
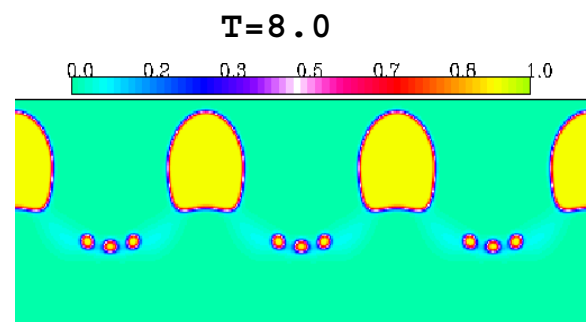
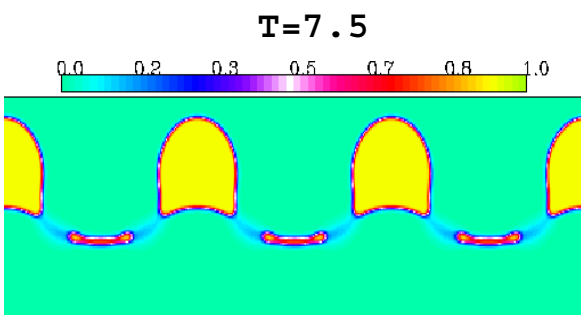
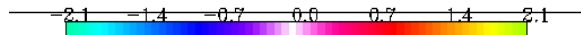
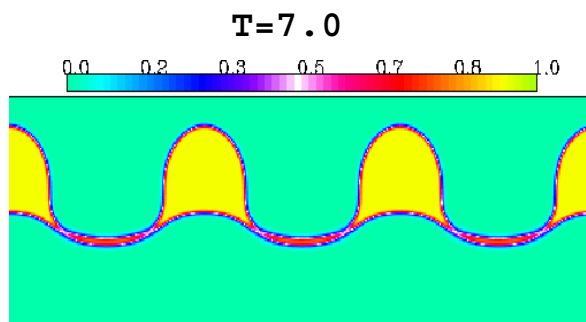
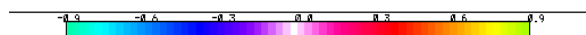
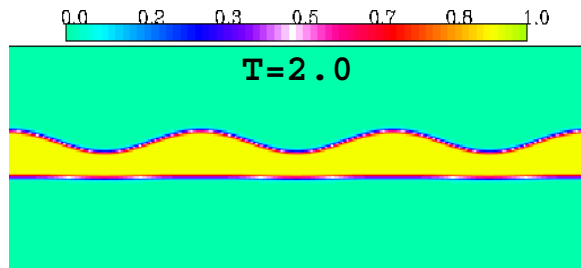
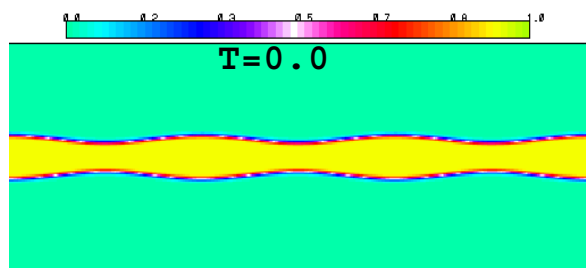


Figure 2:

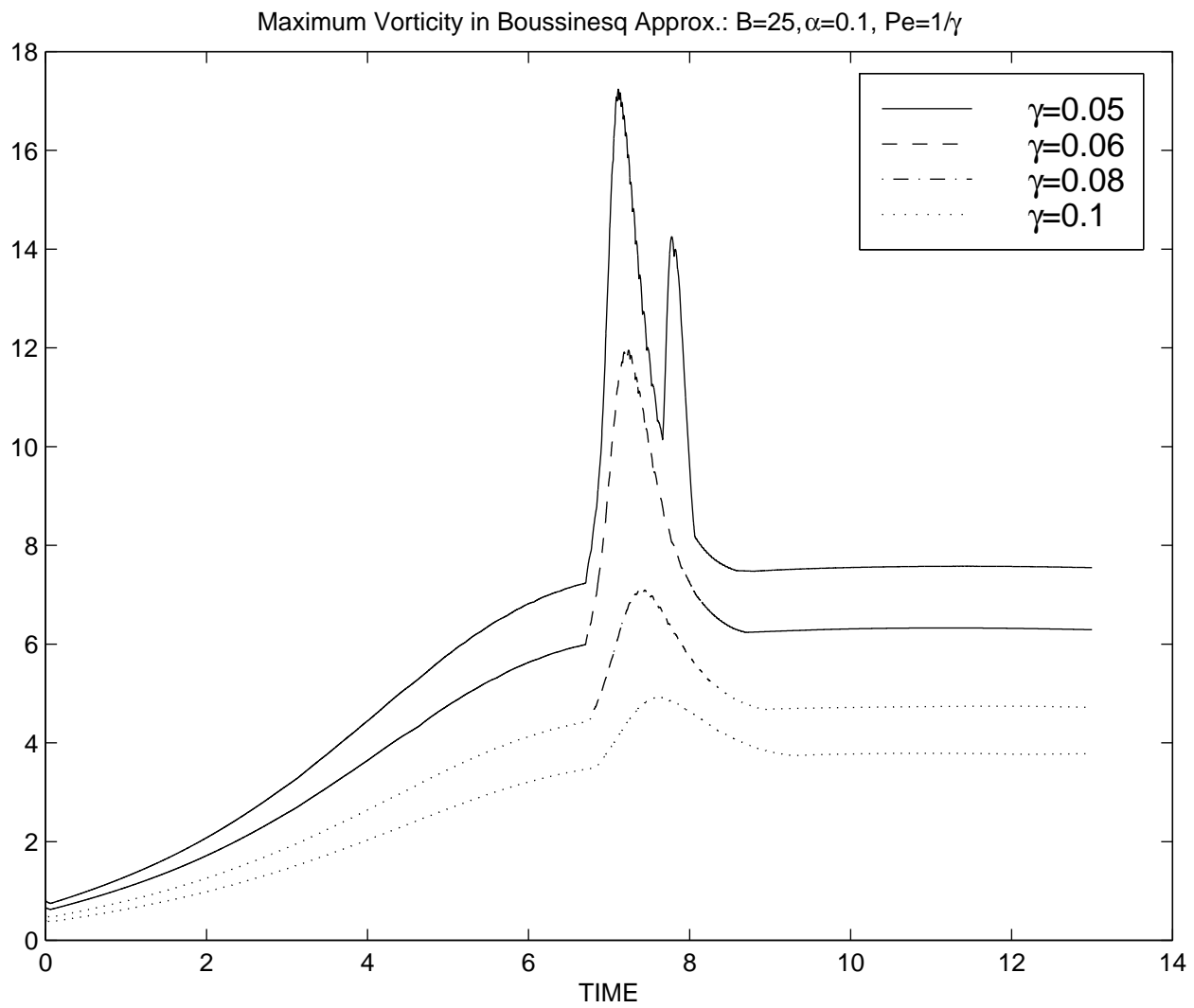


Figure 3:

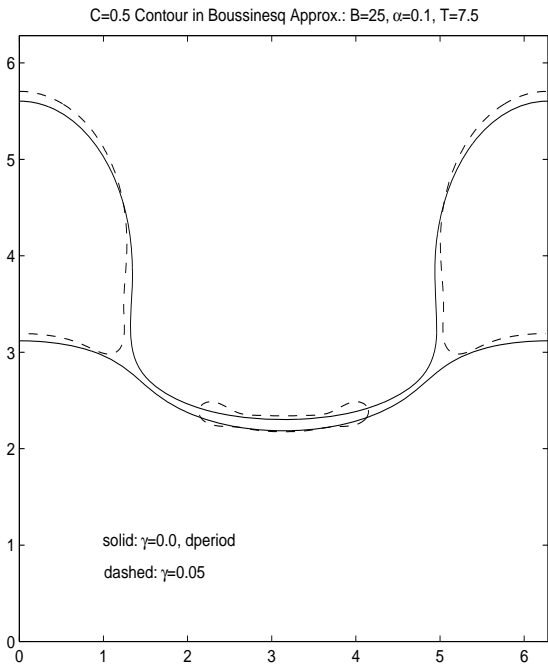
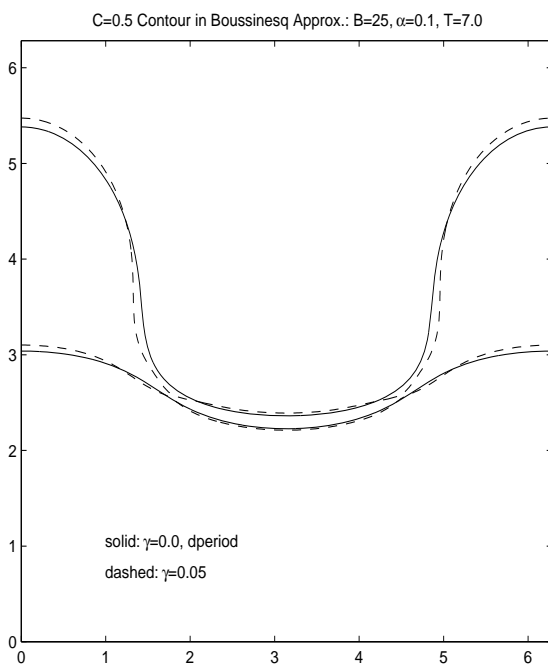
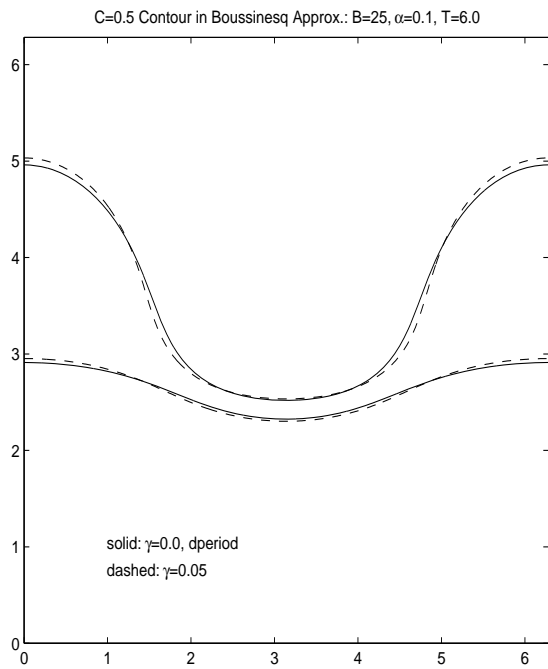
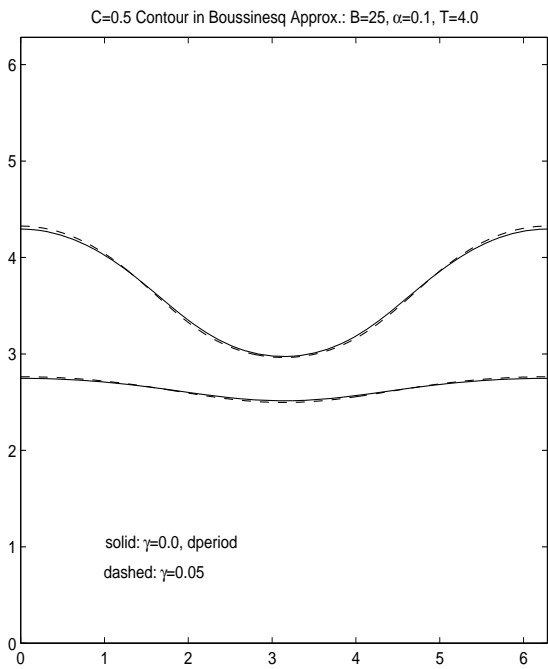
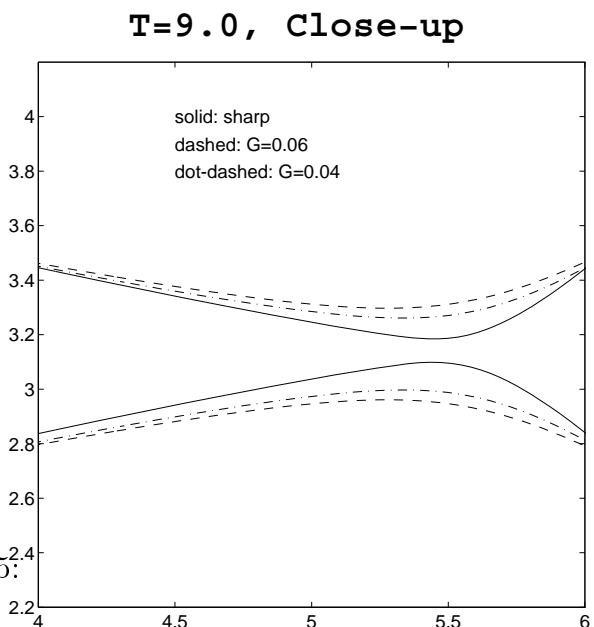
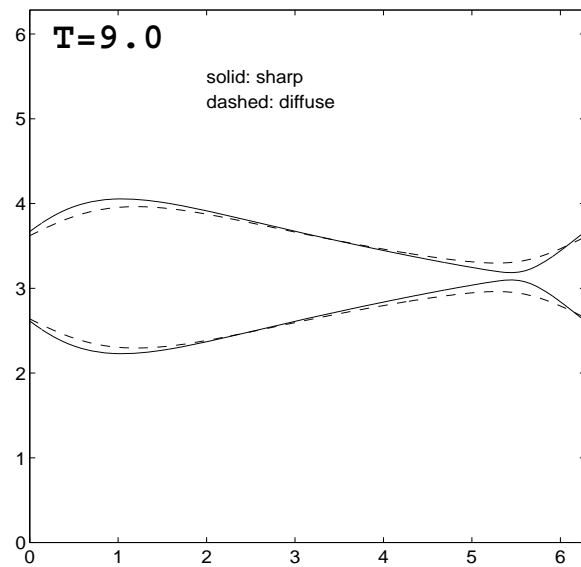
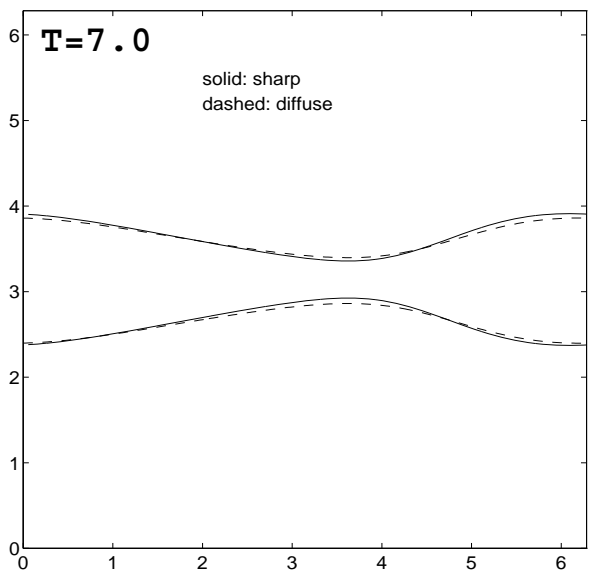
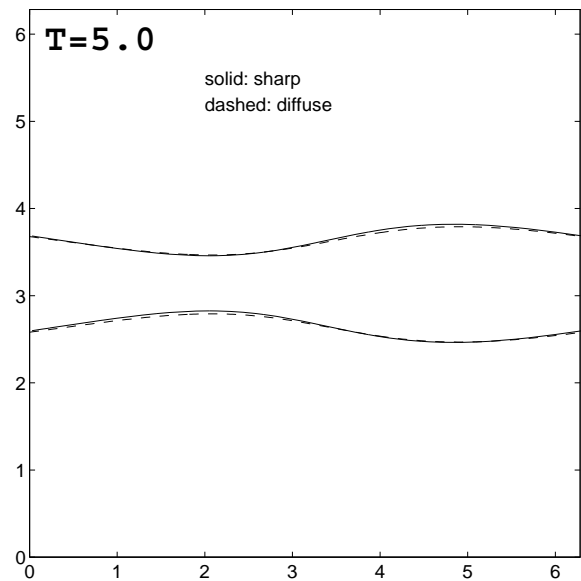
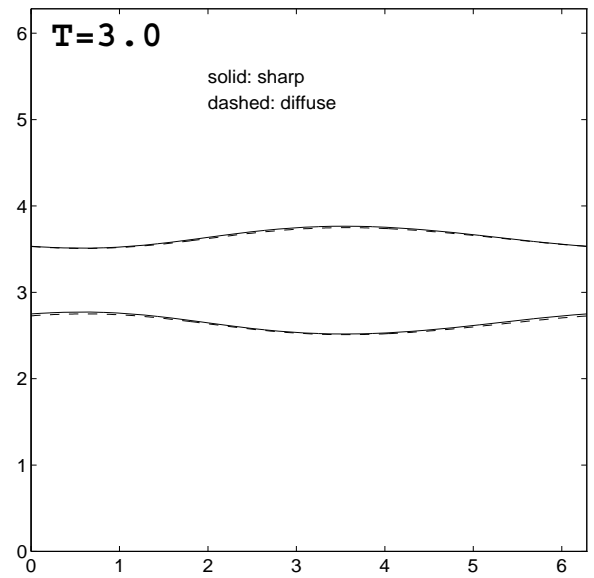
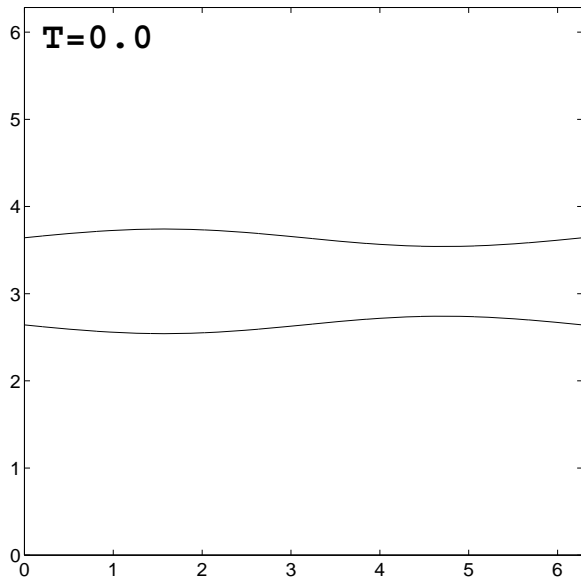
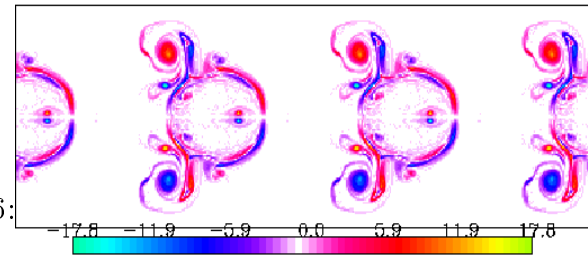
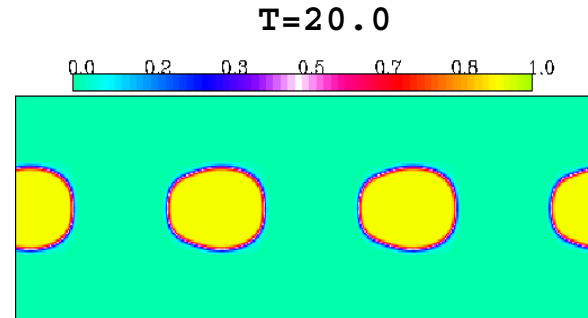
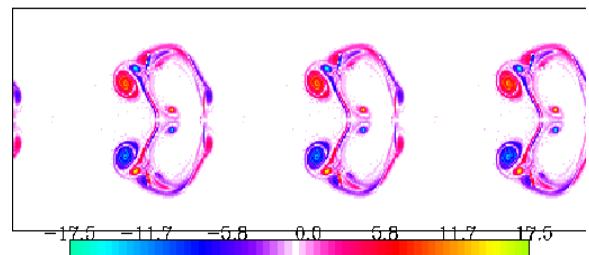
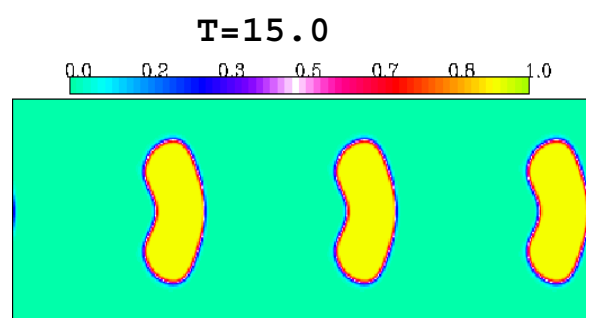
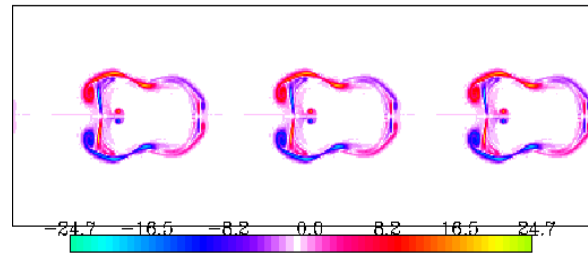
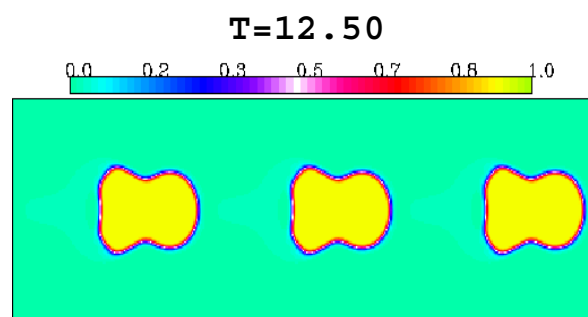
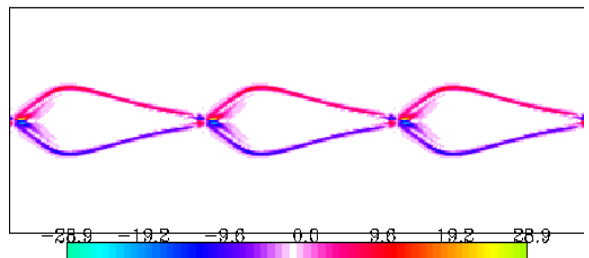
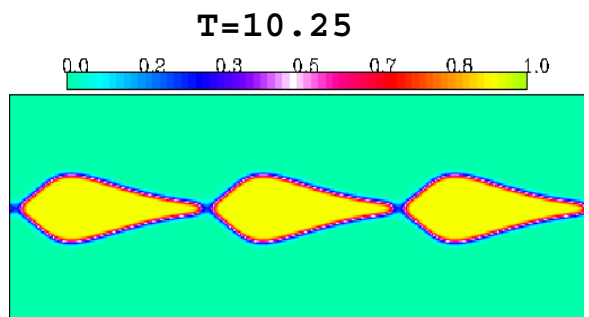
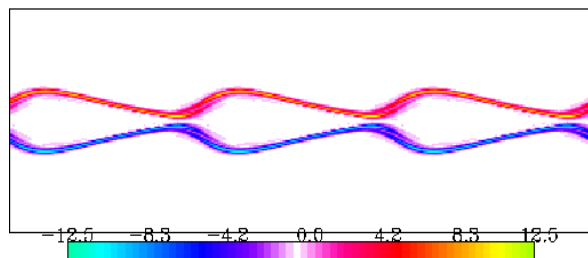
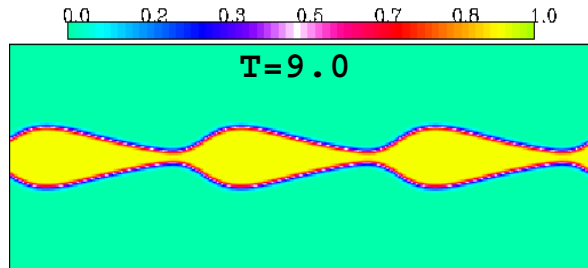
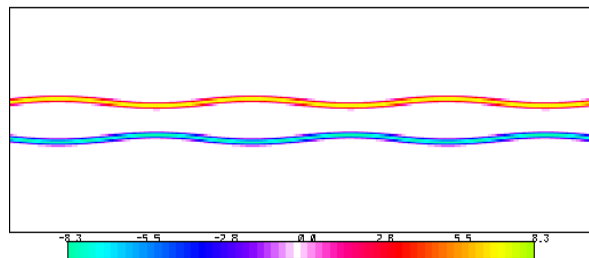
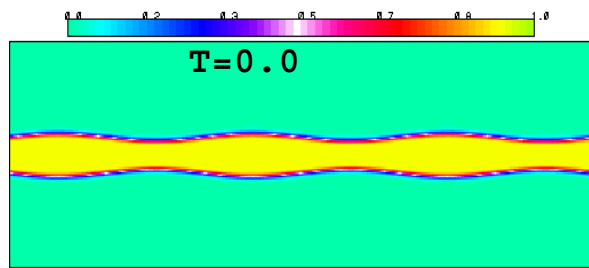


Figure 4:



14
Figure 5:



15
Figure 6: